THE EUROPEAN
PHYSICAL JOURNAL C

CrossMark

Regular Article - Theoretical Physics

Monte Carlo simulations of Higgs-boson production at the LHC with the KrkNLO method

S. Jadach[1]**, G. Nail**[2,3]**, W. Płaczek**[4]**, S. Sapeta**[1,5]**, A. Siódmok**[1,5,a]**, M. Skrzypek**[1]

[1] Institute of Nuclear Physics, Polish Academy of Sciences, ul. Radzikowskiego 152, 31-342 Kraków, Poland
[2] Particle Physics Group, School of Physics and Astronomy, University of Manchester, Oxford Road, Manchester M13 9PL, UK
[3] Institute for Theoretical Physics, Karlsruhe Institute of Technology, Wolfgang-Gaede-Strasse 1, 76131 Karlsruhe, Germany
[4] Marian Smoluchowski Institute of Physics, Jagiellonian University, ul. Łojasiewicza 11, 30-348 Kraków, Poland
[5] Theoretical Physics Department, CERN, Geneva 23 1211, Switzerland

Abstract We present numerical tests and predictions of the KrkNLO method for matching of NLO QCD corrections to hard processes with LO parton-shower Monte Carlo generators (NLO+PS). This method was described in detail in our previous publications, where it was also compared with other NLO+PS matching approaches (MC@NLO and POWHEG) as well as fixed-order NLO and NNLO calculations. Here we concentrate on presenting some numerical results (cross sections and distributions) for Z/γ^* (Drell–Yan) and Higgs-boson production processes at the LHC. The Drell–Yan process is used mainly to validate the KrkNLO implementation in the Herwig 7 program with respect to the previous implementation in Sherpa. We also show predictions for this process with the new, complete, MC-scheme parton distribution functions and compare them with our previously published results. Then we present the first results of the KrkNLO method for Higgs production in gluon–gluon fusion at the LHC and compare them with MC@NLO and POWHEG predictions from Herwig 7, fixed-order results from HNNLO and a resummed calculation from HqT, as well as with experimental data from the ATLAS collaboration.

1 Introduction

The discovery of the Higgs boson, at the Large Hadron Collider (LHC) [1,2], opened a new era in the exploration of the electroweak sector of the standard model (SM). The measured value of the Higgs mass uniquely specifies all of the couplings and turns the SM into a fully predictive theory.

Hence, we are at a position to perform stringent tests of our current modelling of these fundamental interactions. This is only possible if we are in possession of precise theoretical predictions for the Higgs-production cross sections.

Most of the Higgs-boson particles observed at hadron colliders are produced through the process of gluon fusion, a channel that is known to exhibit very slow convergence in perturbative quantum chromodynamics (QCD). At LHC energies, the next-to-leading order (NLO) corrections to the total cross section for the inclusive production of the Higgs boson through gluon fusion turn out to be as large as 70%, and the next-to-next-to-leading order (NNLO) corrections increase the cross section by another 30% [3–5]. The theoretical uncertainty of the NNLO result, arising from the missing higher orders and obtained by the standard renormalization and factorization scale variations, is estimated at around 10%, and is hence at the level of the experimental accuracy of the Run 1 LHC measurements. This large uncertainty at NNLO has motivated the efforts to further improve the precision by calculating the full next-to-next-to-next-to-leading order (N^3LO) result for inclusive Higgs-boson production in gluon fusion [6]. Adding these contributions to the predictions for the cross section reduces their scale uncertainties down to the level of 3%.

Apart from the inclusive Higgs cross section, which is the most fundamental quantity, as it enables one to predict the total number of Higgs particles produced at a given energy and luminosity, one is also equally interested in more differential observables. Therefore, a significant amount of work has also gone into obtaining predictions for differential cross sections for Higgs production in gluon fusion beyond NLO.

In particular, differential observables have been predicted within frameworks of analytic resummation, like for example small-q_T resummation performed in QCD in coordinate

[a] e-mail: andrzej.siodmok@cern.ch

space up to the NNLL+NLO accuracy [7] and directly in momentum space up to NNLL+NNLO [8] as well as within SCET [9] up to NNLL+NLO.

Differential cross sections for Higgs production in gluon fusion have also been widely studied with approaches in which fixed-order NLO results are matched to parton shower (NLO+PS) such as the MiNLO method [10, 11]. Recently, NNLO+PS matched results were computed with the UN^{2}LOPS technique [12] as well as with an extended version of MiNLO [13–15] combined with the HNNLO program [5,16]. The current methods of performing NNLO+PS [11,14,15,17–21] represent clear progress in the matching of fixed-order NNLO QCD calculations with parton-shower Monte Carlos (PSMCs). The next challenge towards even higher-precision perturbative QCD calculations, needed until the end of the LHC era two decades from now, is the combination of the fully exclusive NNLO corrections for the hard process with NLO parton shower (NNLO+NLOPS).

In this article, we present NLO+PS predictions for various differential distributions computed with the KrkNLO approach [22,23]. The main advantage of the KrkNLO method with respect to other methods of matching the fixed-order NLO calculations with PSMCs (MC@NLO and POWHEG) is its simplicity, which stems from the fact that the entire NLO corrections are implemented using a simple, positive, multiplicative MC weight in combination with pre-calculated MC-scheme PDFs. The present work is relevant for the above future developments in the sense that it presents a simplified method of correcting the hard process to NLO level in combination with a leading-order (LO) parton shower (PS) that will hopefully pave the way to NNLO hard processes combined with a NLO PSMC; NLOPS is a parton-shower MC implementing the NLO evolution kernels in the fully exclusive form, thus providing the full set of the soft-collinear counter-terms for the hard process. Reference [24] reviews several feasibility studies which show that constructing such a NLOPS is, in principle, plausible. In our opinion, any simplifications of the NLO+PS matching, as in the KrkNLO method, will be instrumental in the progression towards more ambitious fully exclusive NNLO+NLOPS projects.

The KrkNLO method was first introduced Ref. [25] for Z/γ^* production in hadron collisions (the Drell–Yan process, DY) and was also presented in Ref. [23]. These developments followed the initial study in Refs. [22,26] on the inclusion of fixed-order NLO QCD corrections to the hard process in LO PSMC through an appropriate Monte Carlo weight. This study was performed with the use of some dedicated toy-model parton-shower generator and for gluonstrahlung from quarks only, albeit for two processes: DY production and deep-inelastic electron–proton scattering (DIS).

The first realistic numerical results (total cross sections and distributions of Z/γ^* transverse momentum and rapidity) of the KrkNLO method, based on its implementation in the Sherpa [27] PSMC, were presented in Ref. [25] for the DY process. The KrkNLO results were compared with the fixed-order NLO predictions of MCFM [28] and those of other NLO-PSMC matching methods, namely MC@NLO [29,30] and POWHEG [31,32], as well as with the fixed-order NNLO calculations of DYNNLO [33]. A satisfactory agreement with other NLO calculations was found. Moreover, for the boson transverse momentum the agreement with the NNLO predictions was better than for MC@NLO and POWHEG, which may be explained by effects beyond NLO accounted for in KrkNLO as a result of using the MC factorization scheme and multiplicative virtual+soft-real corrections; see Ref. [25] for more details. In that paper the advantages of the KrkNLO method over the MC@NLO and POWHEG techniques were also discussed.

In Ref. [25] the concept of the Monte Carlo (MC) factorization scheme was introduced as a necessary ingredient of the KrkNLO method; this was further developed in Ref. [34]; see also Ref. [35]. Appropriate MC-scheme parton distribution functions (PDFs) were defined and constructed from PDFs in the standard $\overline{\text{MS}}$ scheme. However, those MC-scheme PDFs included only contributions from parton–parton transitions that were sufficient for the DY process in the NLO approximation—in the following we denote them with MC$_{\text{DY}}$. The complete PDFs in the MC factorization scheme, which include all of the LO parton–parton transitions, were defined, computed and compared with the $\overline{\text{MS}}$ PDFs in Ref. [34], where Higgs-boson production from initial-state gluons was considered. In that paper only the values of the total cross section for the Higgs production at the LHC were shown; further results for this process will be presented in this work. However, before presenting the Higgs results, we first validate the implementation of the KrkNLO method in the Herwig 7 program with respect to its previous implementation in Sherpa using the DY process. The Herwig 7 implementation of the KrkNLO method will be our basic platform for its future developments and applications to other processes. Then we will compare the KrkNLO results for the DY process based on the complete MC-scheme PDFs with those where the MC$_{\text{DY}}$ PDFs, as defined in Ref. [25], are used.

For the process of Higgs production in gluon–gluon fusion, we present the results for the total cross section and the distributions of the Higgs transverse momentum and rapidity at the LHC. The predictions of the KrkNLO method are compared with those of the fixed-order NLO and NNLO calculations of HNNLO [5], the results of the NLO-PSMC matching approaches of MC@NLO [30] and POWHEG [31,32], as well as resummed calculations from HqT [7,36]. We also

confront the predictions of all the above matching methods with the LHC data of the ATLAS experiment [37].

The outline of this paper is the following: In Sect. 2, after describing the set-up for our numerical computations, we present and discuss the results of the KrkNLO method; we do this first for the DY process and then for Higgs production in gluon–gluon fusion at the LHC. Section 3 concludes our work and provides some outlook for future developments. In Appendix A we present comparisons of various PDF parametrizations in the $\overline{\text{MS}}$ and MC factorization schemes.

2 Numerical results

2.1 Set-up

For the numerical evaluation of the cross sections[1] at the LHC for the proton–proton collision energy of $\sqrt{s} = 8\,\text{TeV}$ we have chosen the following set of the Standard Model input parameters:

$$
\begin{aligned}
M_Z &= 91.1876\,\text{GeV}, & \Gamma_Z &= 2.4952\,\text{GeV}, \\
M_W &= 80.4030\,\text{GeV}, & \Gamma_W &= 2.1240\,\text{GeV}, \\
M_H &= 126\,\text{GeV}, & m_t &= 173.2\,\text{GeV}, \\
& & G_\mu &= 1.16637 \times 10^{-5}\,\text{GeV}^{-2},
\end{aligned}
\tag{2.1}
$$

and use the G_μ scheme [38] for the electroweak sector of the Standard Model. We take the renormalization and factorization scales to be $\mu_R^2 = \mu_F^2 = M_B^2$, where M_B is the mass of the Z or Higgs boson for the respective processes. In the case of the Drell–Yan process, detector acceptance cuts are imposed only on the invariant mass of the final-state lepton pair (Z/γ^*-boson):

$$
50\,\text{GeV} < M_{l\bar{l}} < 150\,\text{GeV}. \tag{2.2}
$$

For the Higgs-production process we do not apply any cuts, and for simplicity we set the Higgs boson to be stable. The LO, NLO and NNLO Higgs-production matrix elements are calculated in the $m_t \to \infty$ and $m_{q \neq t} = 0$ approximation. To compute the hadronic cross section, we employ $\overline{\text{MS}}$ PDFs from the LHAPDF library [39] and their MC-scheme counterparts when using KrkNLO. The value of α_s is chosen to match the value used in the PDFs. The PDF set used is detailed in the relevant subsection.

2.2 Drell–Yan process

The results of the KrkNLO method implemented on top of the Sherpa PSMC [27] for the Drell–Yan process were already presented in Ref. [25]. As with these results, for this process we use the MSTW2008 LO set of parton distribution

---

[1] Unless stated otherwise in the text.

Table 1 Values of the total cross section with statistical errors at the Born level for the Drell–Yan process with PDFs in the $\overline{\text{MS}}$ factorization scheme

	MCFM	Sherpa	Herwig 7
σ_{tot} [pb]	936.9 (1)	937.2 (2)	936.6 (2)

functions [40], which has $\alpha_s(M_Z^2) = 0.13938690$. Here we use these Sherpa results to validate a new implementation of KrkNLO in the Herwig 7 program [41,42]. This version of the Herwig 7 PSMC features a new parton-shower algorithm based on the Catani–Seymour (CS) dipole [43] formalism, and is therefore well suited to the implementation of the KrkNLO method. Details on how to implement the KrkNLO method in the CS-dipole PSMC are given in Ref. [25] for the DY process and in Ref. [34] for the Higgs-boson production. In short, it amounts to replacing the $\overline{\text{MS}}$ PDFs with the MC-scheme PDFs and applying to each event generated by the PSMC an appropriate Monte Carlo weight that introduces the NLO QCD correction to a given hard process. This weight is positive-definite and can be computed simply from information provided in an event record.

2.2.1 LO results

As a basis for this validation, we first compare the LO-level predictions from MCFM and Sherpa with those of Herwig 7 using an identical choice of parameters (see Sect. 2.1). The results for the total cross section presented in Table 1 show a very good agreement (within statistical errors) between different programs.

Since the KrkNLO method depends on details of the parton-shower algorithm[2] both dipole showers [44,45] have to be set as similar as possible. The level of agreement of the two PSMCs is presented in Fig. 1, where we show distributions of the final-state e^+e^--pair (the decay product of Z/γ^*-boson) transverse momentum p_{Tee}, invariant mass m_{ee} and rapidity y_{ee}. We can see that all of the distributions are in good agreement. In the case of the transverse-momentum distribution there are some differences at small p_T that result from different treatment of intrinsic-k_T and the soft-parton limit in the two programs, where differences in the latter emerge from the different ordering variables employed in the two programs. The differences at high p_T are due to limited statistics in this region.

---

[2] For example, in Sherpa the initial-state parton shower has a prefactor of $1/2$ in the scale of the running α_s in the calculation of the Sudakov form factor.
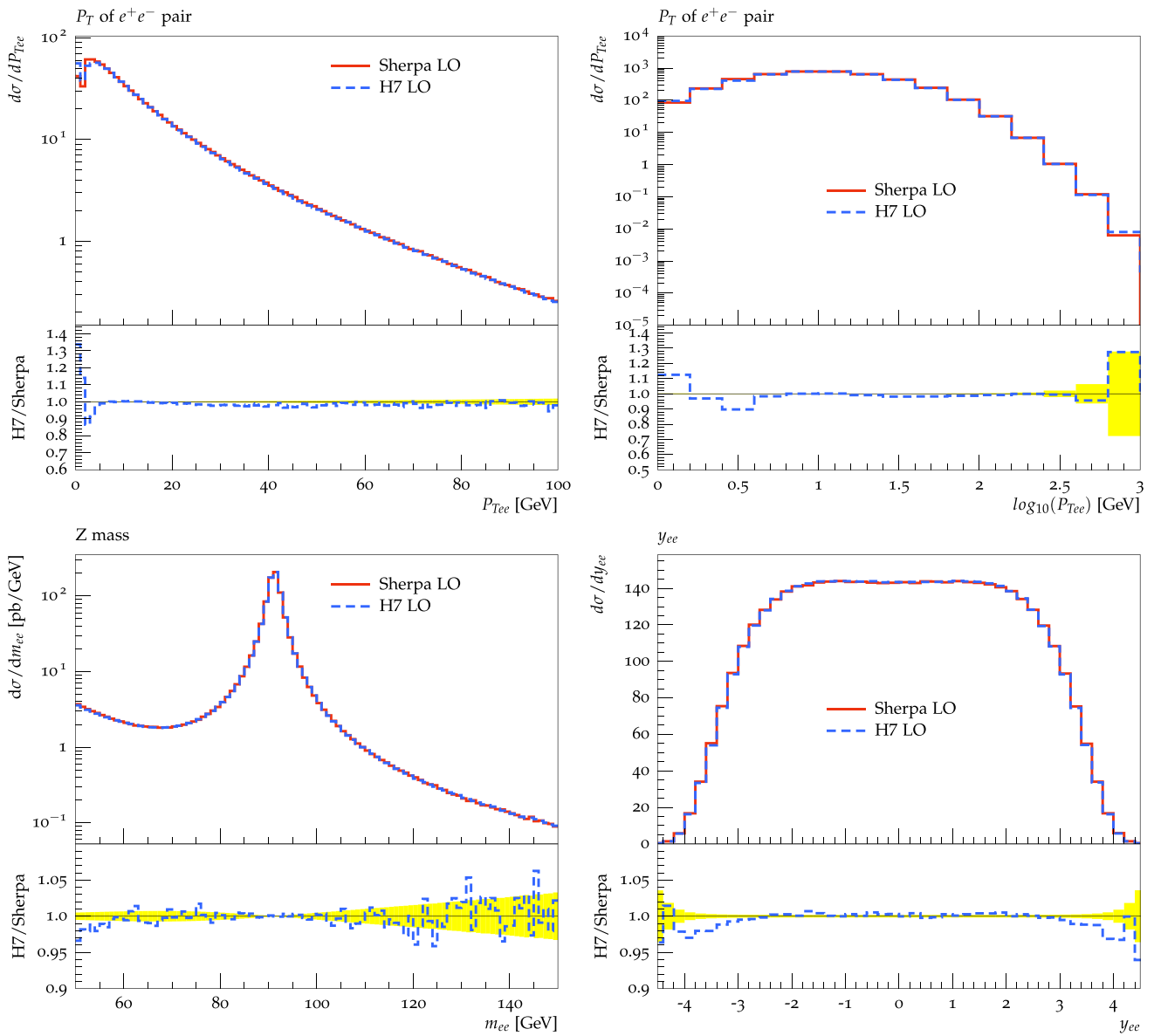
Fig. 1 Comparisons of the Z/γ^* distributions from Sherpa and Herwig 7 for the LO-level Drell–Yan process with e^+e^- pairs in the final state

2.2.2 KrkNLO results: H7 vs. Sherpa implementations

With the consistent predictions obtained at the LO level, we are now ready to examine the consistency between the Sherpa and Herwig 7 implementations of KrkNLO. For the comparisons, we consider both the $q\bar{q}$ and qg NLO channels of the DY process, with the backward evolution of the parton shower running to the end, as in the standard PSMC set-up. In this set-up the argument of α_s in the hard-real NLO corrections is the evolution variable q^2, i.e. $\alpha_s(q^2)$, and in the virtual+soft-real correction it is set to M_Z, i.e. $\alpha_s(M_Z^2)$. Here both programs use the MC$_{DY}$ version of PDFs, those in which only the parton–parton transitions relevant to the DY process up to NLO are considered; see Ref. [25].

Table 2 Values of the total cross section with statistical errors for the Drell–Yan process from the KrkNLO method implemented in Sherpa and Herwig 7 compared to the fixed-order result of MCFM

	MCFM	KrkNLO Sherpa	KrkNLO Herwig 7
σ_{tot} [pb]	1086.5 (1)	1045.2 (3)	1046.5 (2)

Once again, we start from the comparison of the total cross section—the results are collected in Table 2. We see that both implementations of the KrkNLO method give cross sections that agree at the per-mille level—the tiny residual discrepancy is due to the aforementioned differences in the low-p_T region between Herwig 7 and Sherpa which affect the KrkNLO correcting weights. These values also agree with our previous results in Ref. [25] (see Table 5 there).
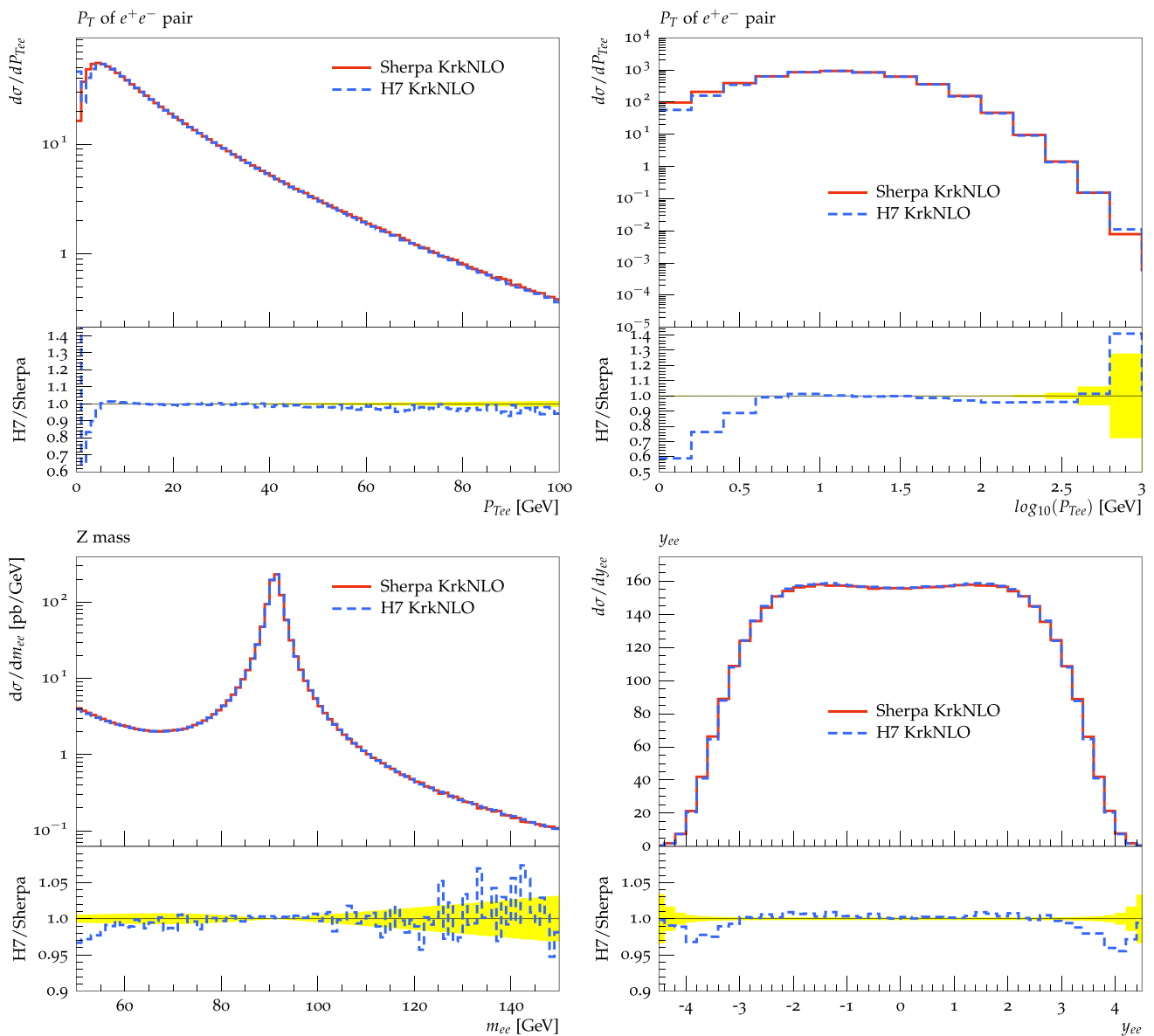
Fig. 2 Comparisons of the Z/γ^* distributions from the KrkNLO method, as implemented in Sherpa and Herwig 7, for the Drell–Yan process with e^+e^- pairs in the final state; see text for details

In Fig. 2, we show similar distributions as in Fig. 1, but this time include the NLO QCD corrections according to the KrkNLO method. Again, a good agreement between the two programs is found. Only in the low p_T region of the p_{Tee} distributions are some differences visible, but they reflect effects already seen in Fig. 1. Given this agreement we are able to validate our implementation of the KrkNLO method in Herwig 7.

2.2.3 KrkNLO results: MC vs. MC_{DY} prescriptions

Having validated the implementation of the KrkNLO method in Herwig 7 we are ready to present the first new results. We start from the comparison of the KrkNLO predictions

based on the MC_{DY} PDFs, defined in Ref. [25], with those in which the complete MC-scheme PDFs, first introduced in Ref. [34], are used. The main difference between the MC_{DY} and MC PDFs is that in the former only the quark PDFs are transformed from the $\overline{MS}$ to MC scheme and the gluon PDF is unchanged, whereas in the latter the gluon PDF is also transformed to the MC scheme; this is described in Ref. [34].

We note that for the DY process the transformation of the gluon PDF comes as an effect beyond NLO, so formally, for any predictions at the NLO level, the MC_{DY} PDFs are sufficient. However, this is not the case for processes in which initial-state gluons are present at the LO level, as is the case for Higgs-boson production in gluon–gluon fusion.

Therefore, for future applications of the KrkNLO method to a generic process we shall use the complete MC PDFs of Ref. [34].

From Table 3 we see that the differences between the values of the total cross section corresponding to these two variants of the MC-scheme PDFs are rather small, $\sim 2\%$, well within uncertainties of the NLO predictions. For comparison, we also show the fixed-order NLO result obtained from

Table 3 Values of the total cross section with statistical errors for the Drell–Yan process from KrkNLO implemented in Herwig 7 for two variants of MC-scheme PDFs compared with the fixed-order NLO result from MCFM; see text for details

	MCFM: $\overline{MS}$ PDFs	KrkNLO: MC_{DY} PDFs	KrkNLO: MC PDFs
σ_{tot} [pb]	1086.5 (1)	1046.5 (2)	1022.3 (2)

Table 4 Values of the total cross section with statistical errors (in brackets) at the LO level for Higgs production in gluon–gluon fusion at the LHC for the $\overline{MS}$ CT10nlo ($\alpha_s = 0.118$) PDFs from HNNLO and Herwig 7 (fixed order); see text for details

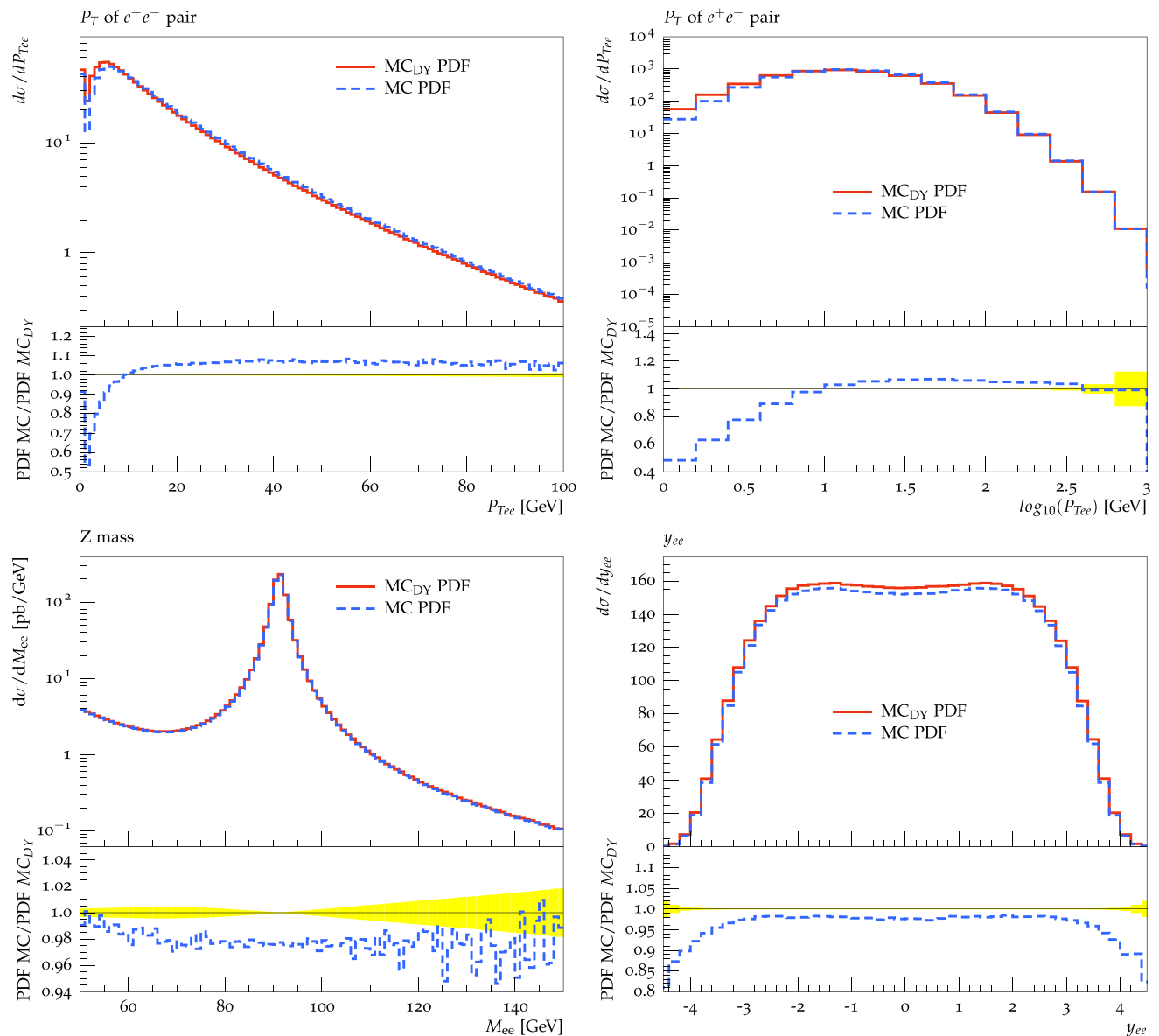|	HNNLO@LO	Herwig 7
σ_{tot} [pb]	5.565 (1)	5.564 (1)

Fig. 3 Comparisons of the Z/γ^* distributions, as in the previous plots, from KrkNLO implemented in Herwig 7 for both the MC_{DY} PDFs and the complete MC PDFs. In the KrkNLO, the NLO weights use $\alpha_s(q^2)$ in the hard-real corrections and $\alpha_s(M_Z^2)$ in the virtual+soft-real ones

Table 5 Values of the NLO total cross section with statistical errors (in brackets) for Higgs-boson production in gluon–gluon fusion at the LHC for KrkNLO, MC@NLO and POWHEG as calculated by Herwig 7, as well as the NLO and NNLO result from HNNLO; see text for details

	MC@NLO	POWHEG		KrkNLO	HNNLO	
		Default	Original		NLO	NNLO
σ_{tot} [pb]	12.700 (2)	12.699 (2)	12.697 (2)	12.939 (2)	12.640 (1)	17.063 (15)

MCFM using the $\overline{\mathrm{MS}}$ PDFs. The differences with respect to the KrkNLO results are at the level of 4–6%, also within the NLO accuracy. For the distributions of the quantities as shown in the previous plots, presented in Fig. 3, the differences are at the level of a few per-cent, except for in the low p_T region where they can grow up to $\sim 50\%$, but this region is very sensitive to soft gluon effects (and thus to the gluon PDF) that are formally beyond the NLO approximation.

2.3 Higgs-boson production

In this section we present results for Higgs-boson production in gluon–gluon fusion at the LHC obtained with the KrkNLO method implemented in Herwig 7 and compare them with predictions of other NLO-PSMC matching approaches, namely MC@NLO [30] and POWHEG [32] as implemented in Herwig 7, as well as with fixed-order calculations at NLO and NNLO from HNNLO [5] and an NNLL+NNLO calculation from HqT [7,36]. We opt to use the `CT10nlo` PDF set [46] which has $\alpha_s(M_Z^2) = 0.118$, and set Herwig 7 equivalently, such that we have a consistent α_s setting across all predictions.[3]

Finally, we confront the theoretical predictions of all the above matching methods with experimental measurements performed at the LHC during Run 1 by the ATLAS collaboration [37].

2.3.1 LO results

We start from the numerical cross-check at the LO level of different programs used in our study. In Table 4 we show the results for the total cross section obtained from HNNLO and Herwig 7 (fixed order). These values are in very good agreement, despite small differences in the running of α_s. We are therefore ensured that all of the parameters as well as PDFs used in computation of Higgs-boson production in gluon–gluon fusion are consistently set in these programs.

2.3.2 NLO results

Here we present the results from KrkNLO alongside those of the MC@NLO and POWHEG methods implemented

---

[3] Aside from small differences in the running α_s between HNNLO and Herwig 7.

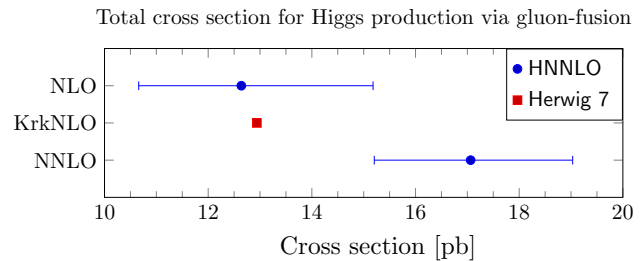Total cross section for Higgs production via gluon-fusion

Fig. 4 Comparison of the total cross section for Higgs-boson production in gluon–gluon fusion at NLO, from HNNLO and KrkNLO, as well as at NNLO from HNNLO. The *error bars*, shown for HNNLO, are obtained from the independent variations of the renormalization and factorization scales by factors of 1/2 and 2 from M_H

in Herwig 7 as well as the NLO and NNLO results from HNNLO as well as a results from HqT. The KrkNLO set-up uses $\alpha_s(q^2)$ for the hard-real corrections and $\alpha_s(M_H^2)$ for the virtual+soft-real corrections. We show two variants of the POWHEG method: The first one, POWHEG (Default), is the default set-up in Herwig 7 and it restricts the transverse momentum of parton-shower emissions to be less than the factorization scale, as is done in the MC@NLO set-up, which follows the initial work of Ref. [29]; the second one, POWHEG (Original), is closer to its original implementation [32] which has no such restriction. This amounts to POWHEG (Default) generating both S and H-events, with POWHEG (Original) only generating S-events.

The values of the total cross section, with statistical errors, for the Higgs-boson production process are shown in Table 5. We can see that, as expected, both the MC@NLO and the POWHEG results give the same total cross sections. The KrkNLO method gives a slightly higher value of the cross section than the other methods. This can be explained by the beyond-NLO contributions that are partially accounted for in the KrkNLO result. Additionally, in Fig. 4 we show the total cross sections from HNNLO, along with error bands generated by the variation of the renormalization and factorization scales by factors of 1/2 and 2 around M_H. We see that the prediction of KrkNLO is within the NLO uncertainty estimate. Furthermore, we see that the uncertainty estimate for NNLO is still rather large, at around 10%, and does not overlap with the NLO range.

In Fig. 5 we present the distributions of the Higgs-boson transverse momentum p_T^{H} and rapidity y_{H}, comparing the results from KrkNLO with the ones from MC@NLO and
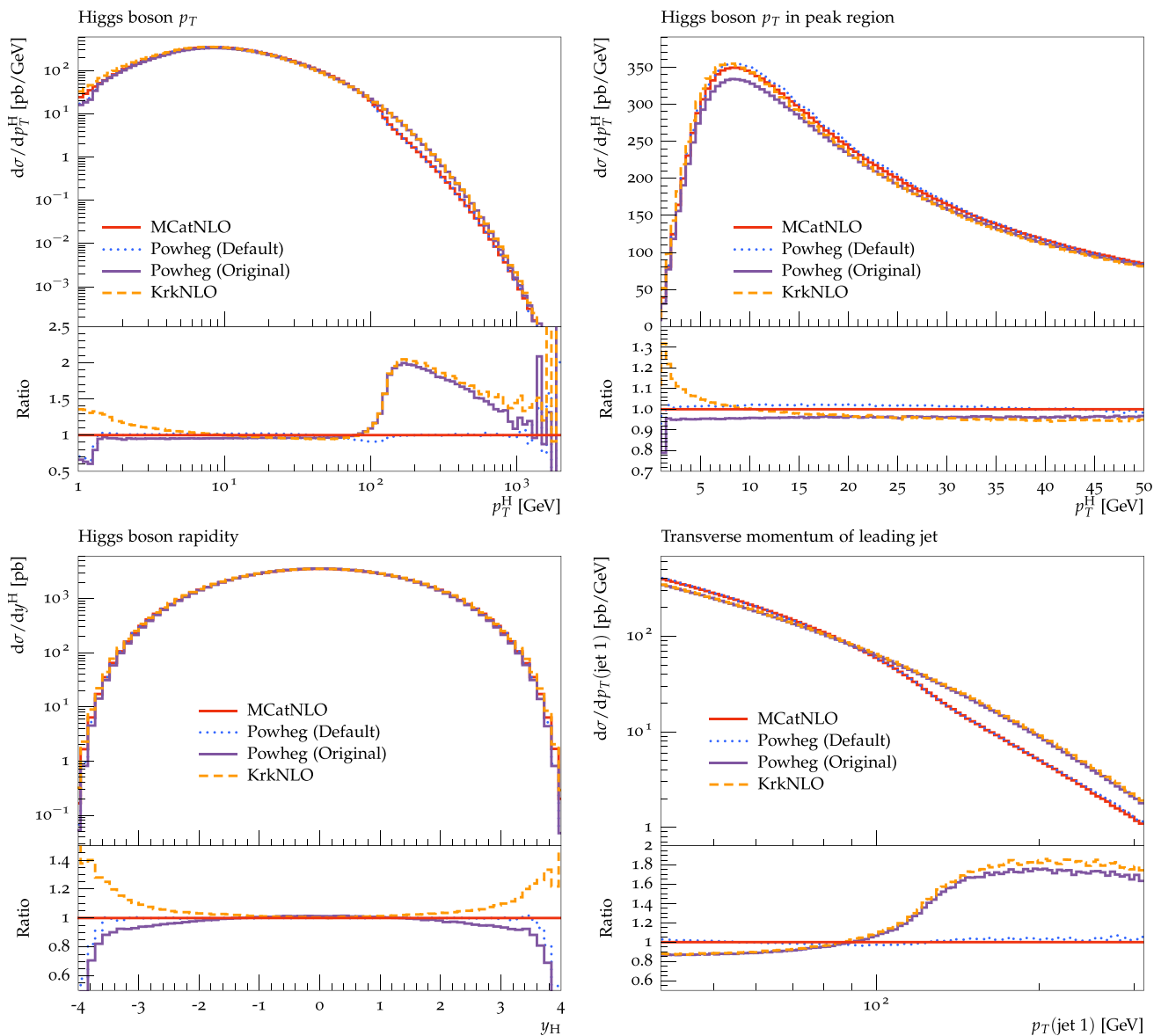
Fig. 5 Comparisons of the Higgs-boson transverse-momentum and rapidity distributions from the KrkNLO, MC@NLO and POWHEG methods implemented in Herwig 7 for Higgs-boson production in gluon–gluon fusion at the LHC; see text for details

POWHEG. All of the predictions agree within a few per-cent for the p_T^H range from ~ 5 GeV to ~ 100 GeV and for the rapidity range $[-3, 3]$. In the region $p_T^H > M_H$ larger differences between KrkNLO and MC@NLO/POWHEG (Default) are visible, whereas KrkNLO produces a similar shape to POWHEG (Original). The main reason for this is that both MC@NLO and POWHEG (Default) restrict the value of the transverse momentum of parton-shower emissions to be below the value of M_H, whereas for KrkNLO, and also POWHEG (Original), there is no such restriction; this can be seen in the upper-left plot, where a sharp drop of the p_T spectrum for $p_T \gtrsim M_H$ is visible in the case where the emissions are restricted by this hard-cutoff. However, this spectrum can be smoothed by relaxing this condition, as shown

in Refs. [47,48]. Of course, such differences are acceptable within the NLO approximation.

Next, in Fig. 6 we compare KrkNLO, MC@NLO and POWHEG predictions from Herwig 7 for the Higgs-boson transverse-momentum distribution with the corresponding result obtained from HNNLO [5,16] and HqT [7,36]. The error bands HNNLO NNLO distributions were obtained by varying the renormalization and factorization scales by the typical factors of $1/2$ and 2 around M_H as an estimate of the uncertainty from neglected higher orders. The HqT distributions were obtained similarly, but also include variations of the resummation scale of $1/2$ and 2 at the central value of $M_H/2$ as recommended in Ref. [36]. The HNNLO comparison, upper plot, is shown relative to the NLO distribution
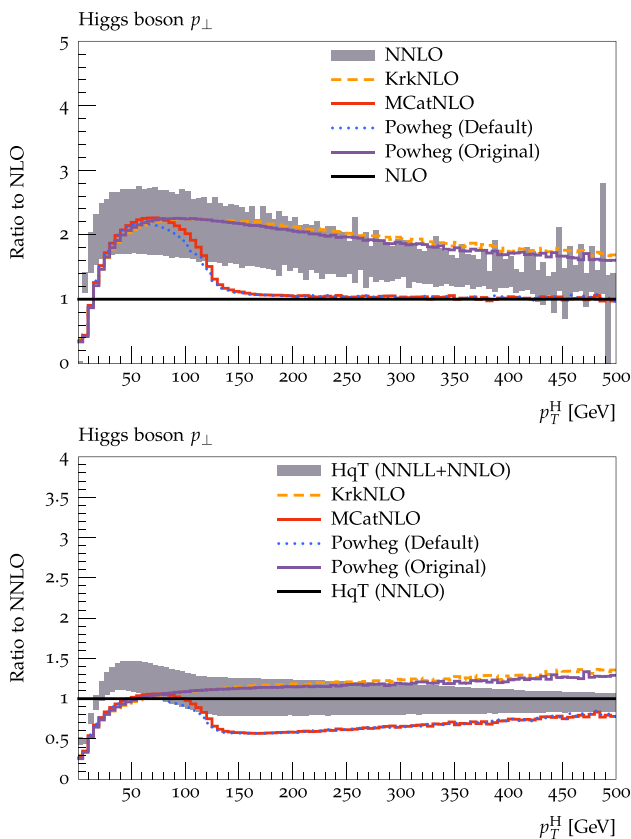
Higgs boson $p_\perp$

Higgs boson $p_\perp$

Fig. 6 Higgs-boson transverse-momentum distributions from KrkNLO, POWHEG and MC@NLO. The *upper plot* compares our results with the fixed-order NNLO result from the HNNLO program and are shown relative to the NLO results from HNNLO. The *lower plot* shows our results in comparison to HqT, these are shown relative to the HqT NNLO prediction. The content of the error bands is described in the main text

from HNNLO and the HqT comparison, lower plot, is shown relative to the NNLO distribution from HqT.

As we see in the upper plot of Fig. 6, both the KrkNLO and the NNLO results show the trends of quickly raising above the NLO result at low and moderate p_T^H and remaining above it at high p_T^H. The fact that our method gives a result that is higher than the NLO one at high p_T^H is a consequence of the mixed real-virtual $\mathcal{O}(\alpha_s^2)$ terms, which constitute part of the NNLO correction and arise because of the multiplicative nature of the KrkNLO approach.

In the upper plot of Fig. 6 we also show similar comparisons with NNLO for MC@NLO and two versions of POWHEG. The behaviour at low p_T^H is close to that from KrkNLO. At high p_T^H, however, MC@NLO and POWHEG (Default), by construction, converge to the NLO results, departing from the NNLO predictions. On the other hand, KrkNLO and POWHEG (Original) are closer to the NNLO predictions but for larger p_T^H values they are marginally harder. The lower plot of Fig. 6 shows results from MC@NLO, POWHEG and KrkNLO compared to the resummed calculation from HqT (for the "switched" option).

All of the NLO+PS give similar results up to roughly 80 GeV. The HqT result peaks towards lower values of p_T^H compared to the other predictions.

In Fig. 7 we show the results of the KrkNLO method obtained for different modern $\overline{\text{MS}}$ PDF sets: CT10nlo (as used in this section), CT14lo, HERAPDF20, MMHT2014lo and NNPDF30lo. Except for CT10, we have used the LO versions of the corresponding PDF parametrizations, since at NLO they become negative at some regions of the x variable and this poses a problem for the Herwig 7 PSMC generator. We can see that the distributions can vary even by up to 40%. The biggest differences are observed at low transverse momenta and large rapidities. In Appendix 1 we compare all the different PDFs in the $\overline{\text{MS}}$ and MC schemes and show that the differences at the level of parton distribution functions; see Fig. 9, are commensurate to those observed in Fig. 7 for the differential cross sections. Further studies of systematic effects due to PDFs are left for the future.

Finally, in Fig. 8 we compare the predictions for the distributions of the Higgs-boson transverse momentum and rapidity, the number of jets and the transverse momentum of the hardest jet from KrkNLO, MC@NLO and POWHEG with the ATLAS data collected in LHC Run 1 with a collision energy of $\sqrt{s} = 8$ TeV [37]. To our generated results for the gluon–gluon fusion we have added the contributions from other Higgs-production channels, denoted XH, taken from Ref. [37]—they account for $\sim 12\%$ of the cross section. All of the data points lie above the theoretical predictions, although the experimental errors are large, The NLO-PSMC matching methods offer largely equivalent predictions with KrkNLO and POWHEG (Original) predicting slightly harder spectrum for high $p_\perp$ and higher rates for larger jet multiplicities (similar trends are also seen in Fig. 5). Further differences were previously discussed in the context of Fig. 5. In our simulations we have used the CT10nlo PDF parametrization, the same that was used in Ref. [37] for theoretical predictions. However, we have checked that changes of our results due to the use of different PDF sets, discussed in Appendix A, are much smaller than the experimental errors of the ATLAS data and negligible compared to the differences between these results and the data points.

3 Conclusions and outlook

In this paper we have presented the numerical results of the KrkNLO method for the Drell–Yan (DY) process and Higgs-boson production in gluon–gluon fusion at the LHC for the collision energy $\sqrt{s} = 8$ TeV.

Firstly, we have validated the implementation of the KrkNLO method in the Herwig 7 PSMC by comparing its results for the DY process with previous results obtained with the Sherpa-based implementation. Then we have presented new results for the DY process with the complete MC-scheme
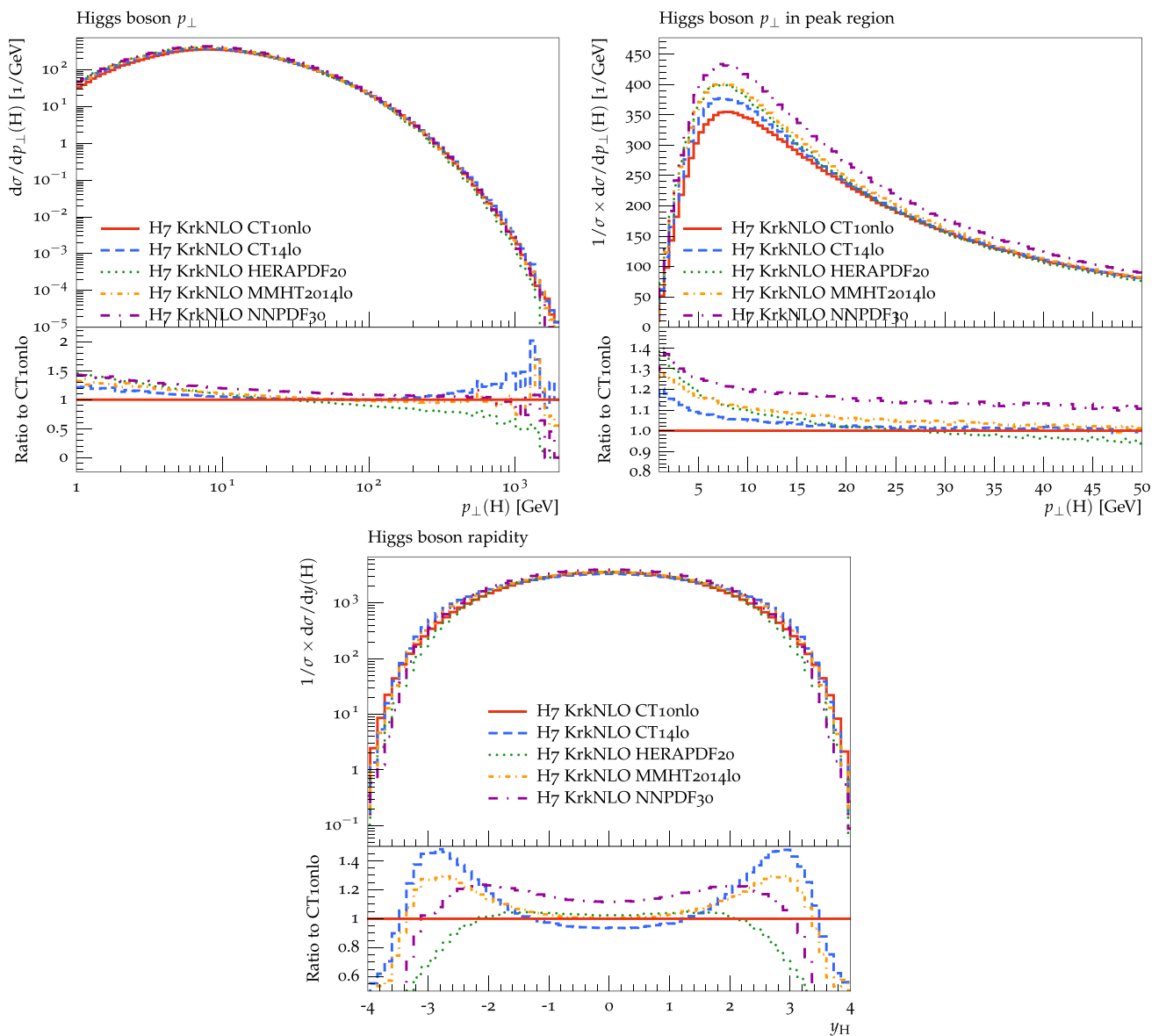
Fig. 7 Comparisons of the Higgs-boson transverse-momentum and rapidity distributions from the KrkNLO method using different PDF sets in the MC factorization scheme for the Higgs-boson production in gluon–gluon fusion at the LHC; see text for details

PDFs that were recently defined in Ref. [34]. These results have been compared with those for the older variant of the MC-scheme PDFs, called here the MC_{DY} PDFs, which were introduced in Ref. [25] exclusively for the DY process. The agreement between the results for these two variants of the MC-scheme PDFs has been found at the level of $\sim 2\%$, which is well within the NLO accuracy.

Our main numerical results in this paper concern the Higgs-boson production process. We have presented the results for the total cross section, as well as distributions of the Higgs-boson transverse momentum and rapidity. The KrkNLO predictions have been compared with those of the MC@NLO and POWHEG methods. A good agreement, within the NLO accuracy, has been found between the default options of these methods. For $p_T^H > M_H$ the KrkNLO result shows better agreement with the POWHEG (Original) option, a result of the restriction on the transverse momentum of the parton-shower emissions to below the factorization scale present in the other set-ups.

Finally, the theoretical predictions of the above NLO-PSMC matching methods have been compared with the ATLAS data from LHC Run 1 for several observables for the Higgs-production process. All of the matching methods underestimate the ATLAS measurements, however, the experimental errors are large. The KrkNLO results offer comparable predictions to other matching methods in all dis-
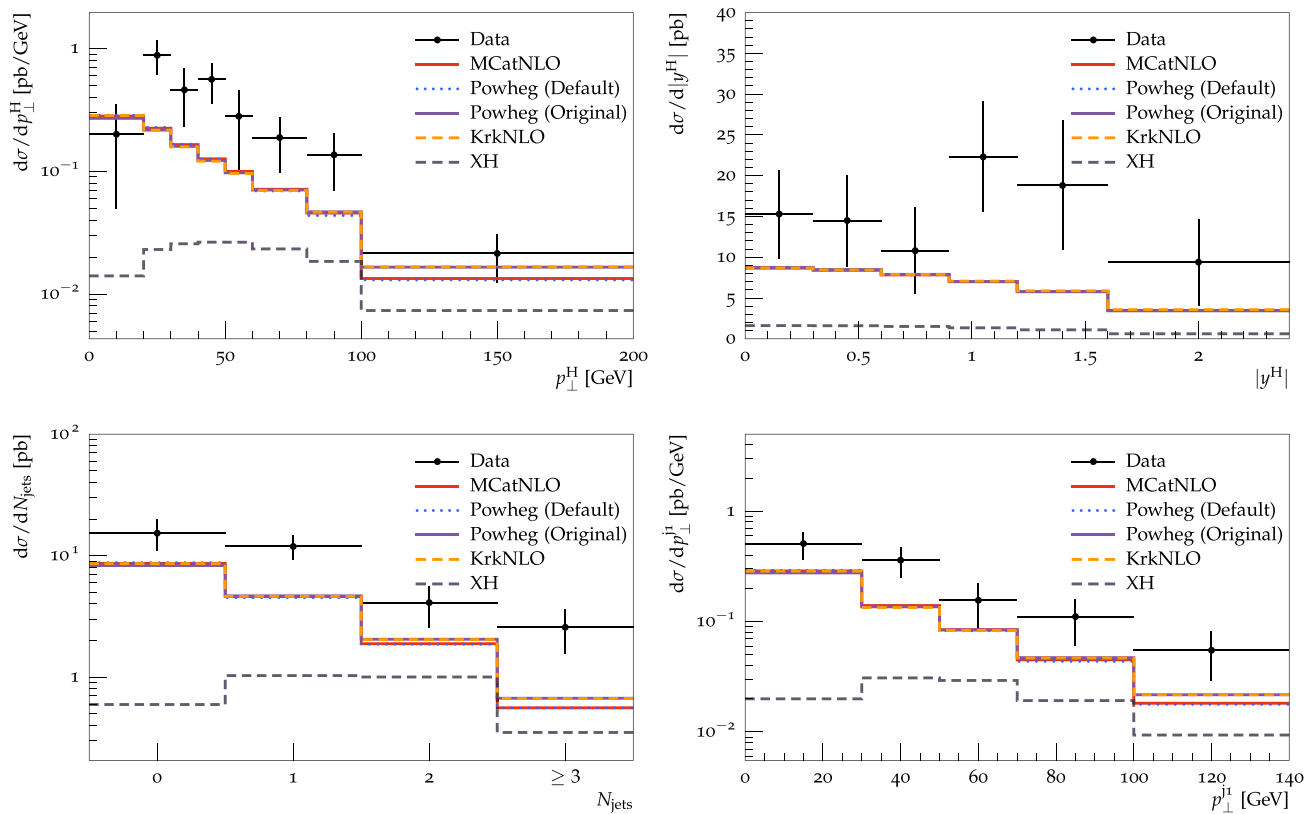
Fig. 8 Comparisons of the predictions of the KrkNLO, MC@NLO and POWHEG methods implemented in Herwig 7 for Higgs-boson production with the ATLAS data from LHC Run 1. The gluon–gluon fusion results from Herwig 7 are plotted on top of the XH results from Ref. [37].

tributions and, along with POWHEG (Original), predict marginally harder spectrum for high p_T and larger jet multiplicities. It is worth mentioning that all the calculations are performed in the infinite top-quark mass approximation, therefore including finite quark mass effects, which are important for large transverse momenta, would most likely bring the predictions closer to the experimental data.

As a next step in our numerical predictions with the KrkNLO method we plan to perform a more detailed study of the Drell–Yan processes, involving both the neutral (Z/γ^*) and the charged ($W^\pm$) modes, in the presence of experimental cuts and a focus on leptonic observables. In order to do this, we need to supplement the NLO-correcting weights with appropriate spin correlations for vector-boson decay products (which is not needed in the case of the scalar Higgs boson). This can be done rather easily within the Herwig 7 PSMC algorithm using the method proposed in Ref. [49]. Future work will seek to apply the KrkNLO method to other processes investigated at the LHC, first of all looking at electroweak-boson pair-production (VV, where $V = \gamma^*, Z, W^+, W^-$) and $V+$jet production. This would be an important test of feasibility and universality of the method.

Future work will also comprise an appraisal of uncertainties of the KrkNLO approach, similar to that of Ref. [50]. Beyond this, the natural extension for KrkNLO is NNLO

+ NLOPS, where NLOPS is PSMC that implements the NLO evolution kernels in the fully exclusive form, and thus provides the full set of the soft-collinear counter-terms for the hard process. Reference [24] reviews several feasibility studies showing that construction of such a NLOPS is, in principle, plausible. Moreover, the simplifications due to the KrkNLO method in achieving NLO+PS will, in our opinion, be instrumental towards these more ambitions research directions.

The KrkNLO project will be available on hepforge at https://krknlo.hepforge.org. This will become the home site of the KrkNLO development, containing relevant codes and the MC-scheme PDFs as well as set-up instructions to facilitate its use within Herwig 7.

Appendix: PDFs in $\overline{\text{MS}}$ and MC schemes

In this appendix we present comparisons of parton the distribution functions used in our study. Figure 9 shows the $\overline{\text{MS}}$ and MC PDFs for the gluon and for the u quark (remaining quark flavours look very similar). The MC PDFs were obtained from the $\overline{\text{MS}}$ sets using the convolutions discussed in Ref. [34].

We observe that the gluon PDF in the MC scheme is larger at small and moderate x than the $\overline{\text{MS}}$ PDF. On the contrary, the quark PDFs are smaller in the MC scheme. We also see that various $\overline{\text{MS}}$ sets exhibit differences that carry on to the MC scheme. These differences lead to a range of predictions shown in Fig. 7.
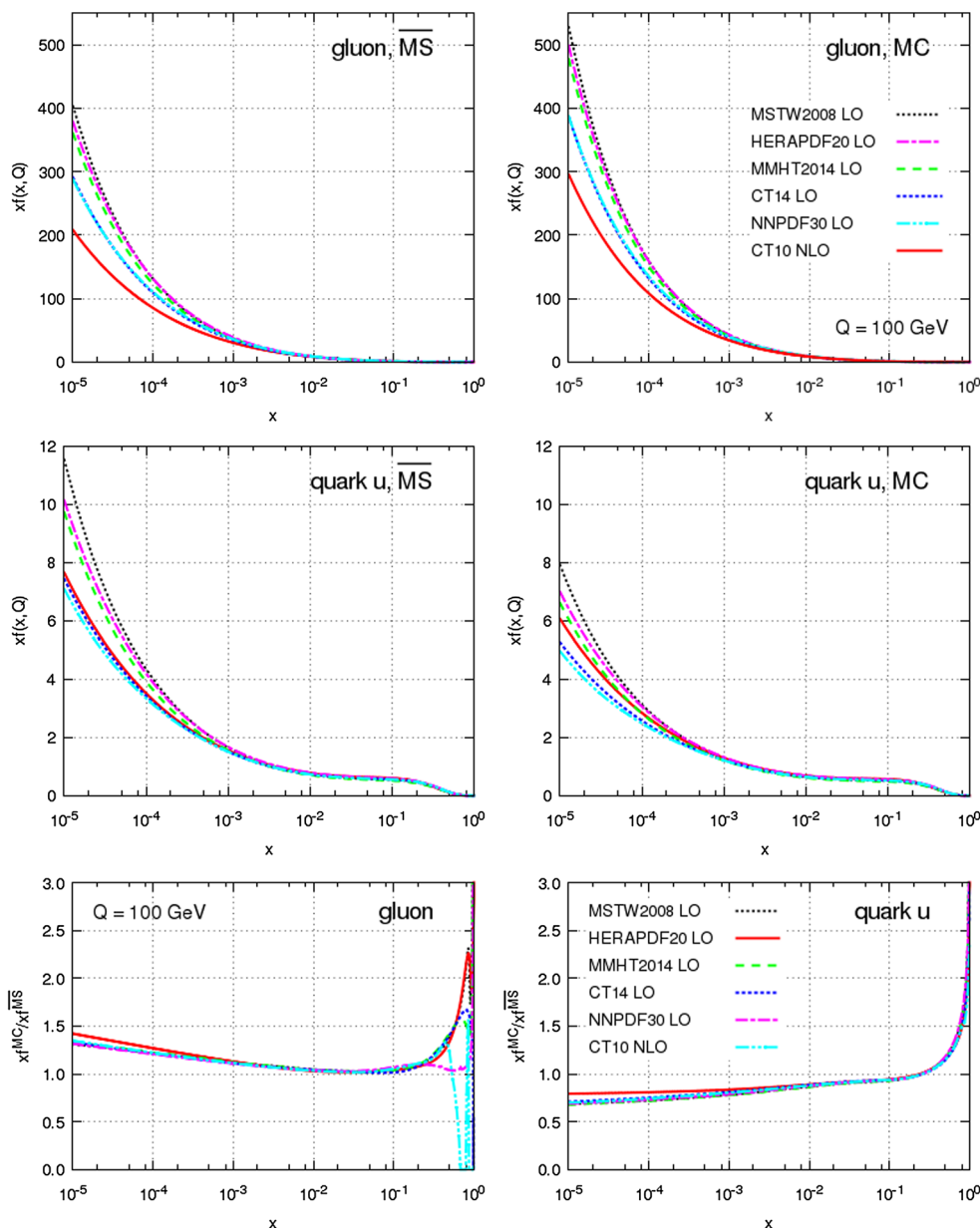

Fig. 9 Comparison of different sets of parton distributions functions in the $\overline{\text{MS}}$ and MC factorization schemes

References

1. ATLAS Collaboration, G. Aad et al., Phys. Lett. B **716**, 1–29 (2012). arXiv:1207.7214
2. CMS Collaboration, S. Chatrchyan et al., Phys. Lett. B **716**, 30–61 (2012). arXiv:1207.7235
3. R.V. Harlander, W.B. Kilgore, Phys. Rev. Lett. **88**, 201801 (2002). arXiv:hep-ph/0201206
4. C. Anastasiou, K. Melnikov, Nucl. Phys. B **646**, 220–256 (2002). arXiv:hep-ph/0207004
5. S. Catani, M. Grazzini, Phys. Rev. Lett. **98**, 222002 (2007). arXiv:hep-ph/0703012
6. C. Anastasiou, C. Duhr, F. Dulat, F. Herzog, B. Mistlberger, Phys. Rev. Lett. **114**, 212001 (2015). arXiv:1503.06056
7. D. de Florian, G. Ferrera, M. Grazzini, D. Tommasini, JHEP **11**, 064 (2011). arXiv:1109.2109
8. P.F. Monni, E. Re, P. Torrielli, Phys. Rev. Lett. **116**(24), 242001 (2016). arXiv:1604.02191
9. T. Becher, M. Neubert, D. Wilhelm, JHEP **05**, 110 (2013). arXiv:1212.2621
10. K. Hamilton, P. Nason, G. Zanderighi, JHEP **1210**, 155 (2012). arXiv:1206.3572
11. K. Hamilton, P. Nason, C. Oleari, G. Zanderighi, JHEP **1305**, 082 (2013). arXiv:1212.4504
12. S. Hoeche, Y. Li, S. Prestel, Phys. Rev. D **90**(5), 054011 (2014). arXiv:1407.3773
13. K. Hamilton, P. Nason, E. Re, G. Zanderighi, JHEP **10**, 222 (2013). arXiv:1309.0017
14. R. Frederix, K. Hamilton, JHEP **05**, 042 (2016). arXiv:1512.02663
15. K. Hamilton, T. Melia, P.F. Monni, E. Re, G. Zanderighi, JHEP **09**, 057 (2016). arXiv:1606.07062
16. M. Grazzini, JHEP **02**, 043 (2008). arXiv:0801.3232
17. S. Hoeche, Y. Li, S. Prestel, arXiv:1405.3607
18. S. Alioli, C.W. Bauer, C. Berggren, F.J. Tackmann, J.R. Walsh et al., JHEP **1406**, 089 (2014). arXiv:1311.0286
19. S. Hoeche, S. Prestel, Eur. Phys. J. C **75**(9), 461 (2015). arXiv:1506.05057
20. S. Alioli, C.W. Bauer, C. Berggren, F.J. Tackmann, J.R. Walsh, Phys. Rev. D **92**(9), 094020 (2015). arXiv:1508.01475
21. K. Hamilton, P. Nason, G. Zanderighi, JHEP **05**, 140 (2015). arXiv:1501.04637
22. S. Jadach, A. Kusina, W. Płaczek, M. Skrzypek, M. Slawinska, Phys. Rev. D **87**, 034029 (2013). arXiv:1103.5015
23. S. Jadach, W. Płaczek, S. Sapeta, A. Siódmok, M. Skrzypek, Acta Phys. Polon. B **46**(11), 2089 (2015)
24. S. Jadach, A. Kusina, W. Płaczek, M. Skrzypek, Acta Phys. Polon. B **44**(11), 2179–2187 (2013). arXiv:1310.6090
25. S. Jadach, W. Płaczek, S. Sapeta, A. Siodmok, M. Skrzypek, JHEP **10**, 052 (2015). arXiv:1503.06849
26. S. Jadach, M. Jeżabek, A. Kusina, W. Płaczek, M. Skrzypek, Acta Phys. Polon. B **43**, 2067 (2012). arXiv:1209.4291
27. T. Gleisberg et al., JHEP **02**, 007 (2009). arXiv:0811.4622
28. J.M. Campbell, R.K. Ellis, Phys.Rev. D **60**, 113006 (1999). http://mcfm.fnal.gov. arXiv:hep-ph/9905386
29. S. Frixione, B.R. Webber, JHEP **06**, 029 (2002). arXiv:hep-ph/0204244
30. S. Frixione, B.R. Webber, arXiv:hep-ph/0601192
31. P. Nason, JHEP **11**, 040 (2004). arXiv:hep-ph/0409146
32. S. Frixione, P. Nason, C. Oleari, JHEP **0711**, 070 (2007). arXiv:0709.2092
33. S. Catani, L. Cieri, G. Ferrera, D. de Florian, M. Grazzini, Phys. Rev. Lett. **103**, 082001 (2009). arXiv:0903.2120
34. S. Jadach, W. Płaczek, S. Sapeta, A. Siodmok, M. Skrzypek, arXiv:1606.00355
35. S. Jadach, W. Płaczek, S. Sapeta, A.K. Siodmok, M. Skrzypek, PoS **LL2016**, 020 (2016). arXiv:1607.00919
36. G. Bozzi, S. Catani, D. de Florian, M. Grazzini, Nucl. Phys. B **737**, 73–120 (2006). arXiv:hep-ph/0508068
37. ATLAS Collaboration, G. Aad et al., Phys. Rev. Lett. **115**(9), 091801 (2015). arXiv:1504.05833
38. G. Altarelli, M.L. Mangano, Proccedings of the workshop on standard model physics (and more) at the LHC. Yellow Report, CERN, 2000–04, 9 (2000)
39. M.R. Whalley, D. Bourilkov, R.C. Group, arXiv:hep-ph/0508110
40. A.D. Martin, W.J. Stirling, R.S. Thorne, G. Watt, Eur. Phys. J. C **63**, 189–285 (2009). arXiv:0901.0002
41. M. Bahr, S. Gieseke, M. Gigg, D. Grellscheid, K. Hamilton et al., Eur. Phys. J. C **58**, 639–707 (2008). arXiv:0803.0883
42. J. Bellm et al., Eur. Phys. J. C **76**(4), 196 (2016). arXiv:1512.01178
43. S. Catani, M.H. Seymour, Nucl. Phys. B **485**, 291–419 (1997). arXiv:hep-ph/9605323
44. S. Schumann, F. Krauss, JHEP **0803**, 038 (2008). arXiv:0709.1027
45. S. Platzer, S. Gieseke, Eur. Phys. J. C **72**, 2187 (2012). arXiv:1109.6256
46. H.-L. Lai, M. Guzzi, J. Huston, Z. Li, P.M. Nadolsky, J. Pumplin, C.P. Yuan, Phys. Rev. D **82**, 074024 (2010). arXiv:1007.2241
47. J. Alwall, R. Frederix, S. Frixione, V. Hirschi, F. Maltoni, O. Mattelaer, H.S. Shao, T. Stelzer, P. Torrielli, M. Zaro, JHEP **07**, 079 (2014). arXiv:1405.0301
48. J. Bellm, G. Nail, S. Platzer, P. Schichtel, A. Siódmok, arXiv:1605.01338
49. M.H. Seymour, Nucl. Phys. B **436**, 443–460 (1995). arXiv:hep-ph/9410244
50. J. Bellm, S. Platzer, P. Richardson, A. Siódmok, S. Webster, Phys. Rev. D **94**(3), 034028 (2016). arXiv:1605.08256